



LAWRENCE  
LIVERMORE  
NATIONAL  
LABORATORY

UCRL-JC-155314

# **Superconducting High-Resolution X-Ray Spectrometers for Chemical State Analysis of Dilute Samples**

*S. Friedrich, O. B. Drury, T. Funk, D. Sherrell,  
V. K. Yachandra, S. E. Labov, and S. P.  
Cramer*

**September 2, 2003**

8<sup>th</sup> International Conference on Synchrotron Radiation  
Instrumentation, San Francisco, California, August 26-29,  
2003

## DISCLAIMER

This document was prepared as an account of work sponsored by an agency of the United States Government. Neither the United States Government nor the University of California nor any of their employees, makes any warranty, express or implied, or assumes any legal liability or responsibility for the accuracy, completeness, or usefulness of any information, apparatus, product, or process disclosed, or represents that its use would not infringe privately owned rights. Reference herein to any specific commercial product, process, or service by trade name, trademark, manufacturer, or otherwise, does not necessarily constitute or imply its endorsement, recommendation, or favoring by the United States Government or the University of California. The views and opinions of authors expressed herein do not necessarily state or reflect those of the United States Government or the University of California, and shall not be used for advertising or product endorsement purposes.

This is a preprint of a paper intended for publication in a journal or proceedings. Since changes may be made before publication, this preprint is made available with the understanding that it will not be cited or reproduced without the permission of the author.

This report has been reproduced directly from the best available copy.

Available electronically at <http://www.doc.gov/bridge>

Available for a processing fee to U.S. Department of Energy  
And its contractors in paper from  
U.S. Department of Energy  
Office of Scientific and Technical Information  
P.O. Box 62  
Oak Ridge, TN 37831-0062  
Telephone: (865) 576-8401  
Facsimile: (865) 576-5728  
E-mail: [reports@adonis.osti.gov](mailto:reports@adonis.osti.gov)

Available for the sale to the public from  
U.S. Department of Commerce  
National Technical Information Service  
5285 Port Royal Road  
Springfield, VA 22161  
Telephone: (800) 553-6847  
Facsimile: (703) 605-6900  
E-mail: [orders@ntis.fedworld.gov](mailto:orders@ntis.fedworld.gov)  
Online ordering: <http://www.ntis.gov/ordering.htm>

OR

Lawrence Livermore National Laboratory  
Technical Information Department's Digital Library  
<http://www.llnl.gov/tid/Library.html>

# Superconducting High-Resolution X-Ray Spectrometers For Chemical State Analysis Of Dilute Samples

Stephan Friedrich<sup>1,2</sup>, Owen B. Drury<sup>1,2</sup>, Tobias Funk<sup>3</sup>, Darren Sherrell<sup>3</sup>, Vittal K. Yachandra<sup>3</sup>, Simon E. Labov<sup>1</sup>, Stephen P. Cramer<sup>2,3</sup>

<sup>1</sup>*Advanced Detector Group, Lawrence Livermore National Laboratory, L-270, Livermore, CA 94550*

<sup>2</sup>*Department of Applied Science, University of California, Davis, CA, 95616*

<sup>3</sup>*Physics Biosciences Division, Lawrence Berkeley National Laboratory, MS 6-2100, Berkeley, CA 94720*

**Abstract.** Cryogenic X-ray spectrometers operating at temperatures below 1 K combine high energy resolution with broadband efficiency for X-ray energies up to 10 keV. They offer advantages for chemical state analysis of dilute samples by fluorescence-detected X-ray absorption spectroscopy (XAS) in cases where conventional Ge or Si(Li) detectors lack energy resolution and grating spectrometers lack detection efficiency. We are developing soft X-ray spectrometers based on superconducting Nb-Al-AlOx-Al-Nb tunnel junction (STJ) technology. X-rays absorbed in one of the superconducting electrodes generate excess charge carriers in proportion to their energy, thereby producing a measurable temporary increase in tunneling current. For STJ operation at the synchrotron, we have designed a two-stage adiabatic demagnetization refrigerator (ADR) with a cold finger that holds a 3 × 3 array of STJs inside the UHV sample chamber at a temperature of ~0.1 K within ~15 mm of a room temperature sample. Our STJ spectrometer can have an energy resolution below 10 eV FWHM for X-ray energies up to 1 keV, and has total count rate capabilities above 100,000 counts/s. We will describe detector performance in synchrotron-based X-ray fluorescence experiments and demonstrate its use for XAS on a dilute metal site in a metalloprotein.

## INTRODUCTION

Cryogenic x-ray detectors with an operating temperature below 1 K are being developed for applications from material science [1,2,3] and biophysics [4] to particle and astrophysics [5,6] because of their high energy resolution and broadband efficiency. Superconducting tunnel junctions (STJs) are the class of cryogenic detectors preferred for synchrotron applications, since they can be operated at count rates well above those of other low temperature detector technologies [7]. STJs consist of two superconducting electrodes separated by a thin insulating tunnel barrier. They exploit the small energy gap by which excited quasiparticle states are separated from the superconducting electronic ground state constituted by Cooper pairs. A photon with energy  $E$  is absorbed in one of the electrodes, breaks Cooper pairs and thereby generates excess quasiparticles in proportion to its energy. These quasiparticles can tunnel through the insulating barrier, thereby producing an excess current proportional to the energy of the incoming photon. The total charge  $Q$  thus provides a measure of the photon energy according to

$$\frac{Q}{e} = \langle n \rangle \frac{E}{\epsilon} \pm \langle n \rangle \sqrt{\frac{E}{\epsilon} (F + 1 + 1/\langle n \rangle)} \quad (1)$$

Here  $e$  is the electronic charge,  $1.7$  is the average energy required to generate a single excess quasiparticle,  $\langle n \rangle$  is the average number of tunneling events each quasiparticle undergoes, and  $F = 0.2$  is the Fano factor that describes the statistical fluctuations in the initial charge generation process.

Since the energy gap is of order 1 meV in superconductors, about a factor 1000 smaller than the gap in semiconductors, the energy resolution in STJs can theoretically be a factor  $\sqrt{1000} \approx 30$  higher than in Si(Li) or Ge detectors, i.e. well below 10 eV FWHM for photon energies up to 10 keV. The maximum count rate in STJs is set by the average quasiparticle life time, since charges cannot be swept out of a superconductor with a voltage. For typical life times of several  $\mu$ s, count rates above 10,000 counts/s per pixel can be achieved.

## SPECTROMETER DESIGN AND PERFORMANCE

Our STJ detectors are based on vertically stacked Nb-Al-AlOx-Al-Nb thin film technology. They consist of a 165 nm top Nb absorber film, an Al-AlOx-Al tunnel junction whose 50 nm Al electrodes serve as quasiparticle traps, and a 265 nm bottom Nb electrode. Quasiparticles generated in the top Nb absorber diffuse into Al film where the energy gap is lower, scatter inelastically and are then trapped in the region near the tunnel barrier. Each quasiparticle can tunnel multiple times, each time transferring charge in direction of the  $\sim 300 \mu\text{V}$  bias across the barrier. This provides intrinsic charge amplification by an average factor  $\langle n \rangle$ , but also adds statistical noise  $1+1/\langle n \rangle$  due to variations in the average number of tunneling events, and thus affects the ultimately attainable energy resolution. Device sizes vary between  $50 \mu\text{m} \times 50 \mu\text{m}$  and  $200 \mu\text{m} \times 200 \mu\text{m}$  per pixel, with smaller devices typically achieving higher energy resolution because of lower device capacitance, lower leakage currents and fewer Fiske mode resonances [8,9]. For fluorescence-detected absorption spectroscopy of dilute samples at the synchrotron, we trade off some energy resolution for larger solid angle coverage and operate a  $3 \times 3$  array of  $200 \mu\text{m} \times 200 \mu\text{m}$  STJs.

To operate our STJ array at a beam line endstation, we have built a two-stage adiabatic demagnetization refrigerator (ADR) with a 40-cm-long cold finger that holds the STJ array within 15 mm of the room temperature sample inside the UVH chamber (figure 1) [10]. After precooling with liquid nitrogen and liquid helium to 4.2 K, the base temperature below 100 mK is attained by isothermal magnetization and adiabatic demagnetization of two paramagnets [11]. Magnetization lowers the entropy of the paramagnet, and the heat of magnetization is carried into the liquid He bath through a closed heat switch. After opening the heat switch, the magnetic field is decreased sufficiently slowly to keep the entropy of the paramagnet constant, thereby lowering its temperature. The two-stage design uses a gadolinium gallium garnet  $\text{Gd}_3\text{Ga}_5\text{O}_{12}$  (GGG) to cool to 1 K, and  $\text{Fe}(\text{NH}_4)(\text{SO}_4)_2 \times 12 \text{H}_2\text{O}$ , commonly known as FAA for ferric ammonium alum, to cool to a base temperature of  $\sim 80 \text{ mK}$  without having to pump on the liquid helium bath. Our ADRs are compact, reliable and easy to use, and the hold time per magnetization cycle is about 20 hours below 400 mK, the maximum operating temperature of our STJs.

The STJ detector is mounted at the end of an Au-plated OFHC Cu rod that is bolted to the 0.1 K stage at three points for stability and thermal contact. This rod is surrounded by a helium-cooled OFHC Cu radiation shield, which also holds the STJ detector magnet needed to suppress the dc Josephson current for stable STJ operation. All of this is enclosed with a second radiation shield attached to the liquid-N<sub>2</sub>-cooled stage. At the end of the cold finger there are three  $200 \text{ \AA}$  Al on  $1000 \text{ \AA}$  parylene infrared (IR) blocking windows to prevent room temperature radiation from heating the cold stage and causing IR induced excess noise in the detector. Their size is determined by a trade-off between desired angle of acceptance and tolerable IR photon flux.

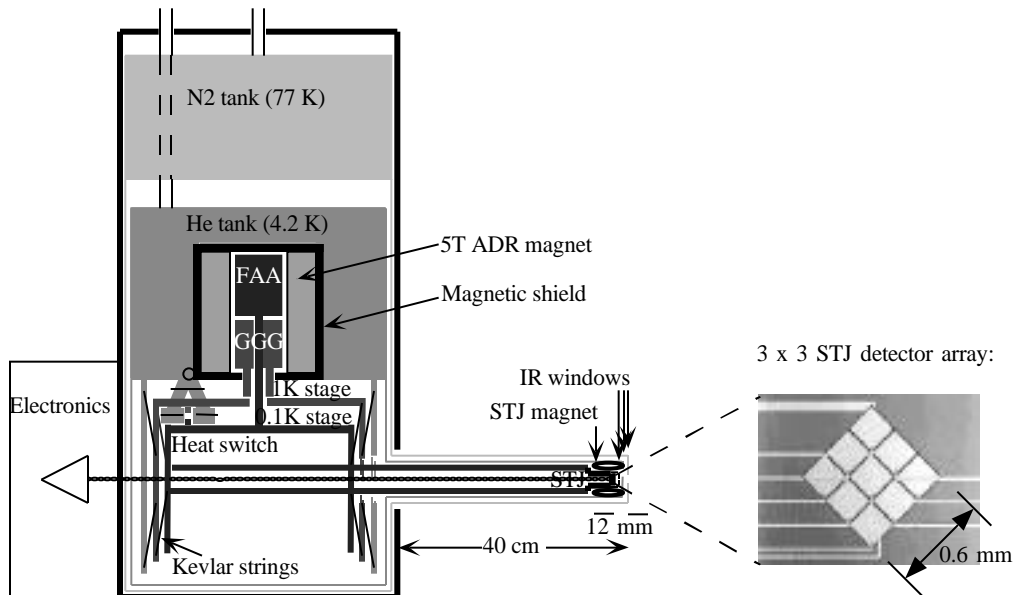


**FIGURE 1.** Superconducting spectrometer design. The detector is held at  $\sim 0.1 \text{ K}$  at the end of the cold finger behind three thin IR-blocking windows. The preamplifier signal can be processed with standard pulse processing electronics.

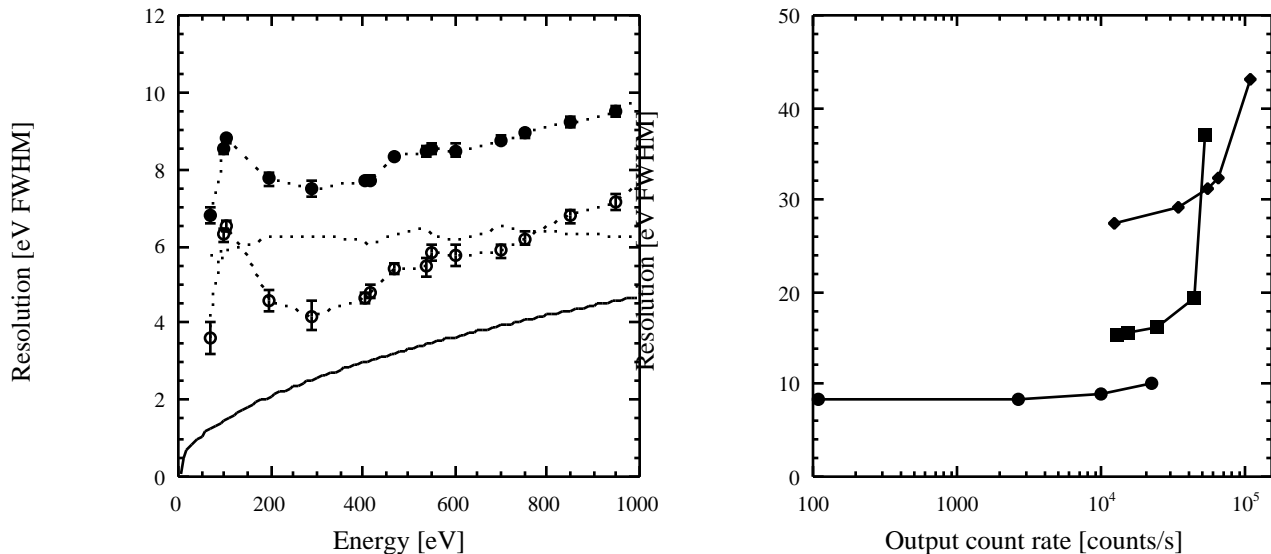


**FIGURE 2.** Left: Energy resolution as a function of energy of a  $100\ \mu\text{m} \times 100\ \mu\text{m}$  STJ detector. The intrinsic device resolution (open circles) is obtained by subtracting the electronic noise (dashed line) from the measured resolution (solid circles) and compared to the theoretical limit according to equation (1) for  $\langle n \rangle = 3.1$  (solid line). Right: Energy resolution at 277 eV for a single STJ pixel as a function of throughput for 4  $\mu\text{s}$  (circles), 1  $\mu\text{s}$  (squares) and 0.25  $\mu\text{s}$  (diamonds) shaping time.

We have illuminated a  $100\ \mu\text{m} \times 100\ \mu\text{m}$  STJ detector directly with monochromatic undulator radiation to test its resolution as a function of energy and count rate (figure 2). The energy resolution varies between 6.8 and 9.5 eV FWHM in the energy band between 50 and 1000 eV, dominated by  $\sim 6$  eV electronic noise. This is somewhat less than the resolution between 1.7 and 8.9 eV of nominally identical STJ detectors mounted in the center of an ADR [8,12], rather than at the end of a cold finger. This discrepancy is likely due to excess noise caused by IR radiation. When subtracting the electronic noise in quadrature from the measured device resolution, we find an intrinsic detector resolution that is within  $\sim 50\%$  of the statistical limit given by equation (1) for  $\langle n \rangle = 3.1$ .

We have examined the high count rate performance of this detector by varying the exit slit size at a constant excitation energy of 277 eV (figure 2). The energy resolution is  $\sim 8$  eV FWHM up to a count rate of  $\sim 10,000$  counts/s for a single pixel at a shaping time of 4  $\mu\text{s}$ . At 22,000 counts/s, the resolution is reduced to 10.2 eV by pile-up. Operation at higher rates is possible, albeit with a shorter shaping time and consequently lower resolution of 19.3 eV at 43,000 counts/s (1  $\mu\text{s}$  shaping) and 42.9 eV at 105,000 counts/s (0.25  $\mu\text{s}$  shaping).

## FLUORESCENCE-DETECTED ABSORPTION SPECTROSCOPY

Synchrotron-based x-ray absorption spectroscopy (XAS) samples atomic energy levels with sub-eV resolution by scanning the energy of a monochromatic beam through an absorption edge of the element of interest. For dilute samples, the sensitivity is highest when recording the intensity of the corresponding x-ray fluorescence as a measure of absorption (fluorescence-detected XAS) [13]. This greatly reduces the number of background counts, provided that the fluorescence line of interest can be separated from neighboring lines in multi-element specimens. Cryogenic x-ray detectors offer an advantage in the soft X-ray energy range below 1 keV whenever conventional Si(Li) or Ge detectors lack energy resolution, and grating spectrometers lack the efficiency to collect X-rays from dilute samples within an acceptable period of time. A short measurement time is crucial for biological samples that suffer from radiation damage.

We demonstrate the sensitivity of the spectrometer with an Mn L-edge absorption spectrum from a dried (and biologically inactive) film of the photosystem II protein, taken at beam line 4.0.2 at the Advanced Light Source [14]. The Mn-cluster in the oxygen-evolving complex of photosystem II is responsible for oxygen evolution in plants, and Mn L-edge spectroscopy can contribute to understanding the enzymatic mechanisms of that process. At constant excitation energy, the response of the nine channels in the array is quite homogeneous, and the weak Mn L fluorescence at  $\sim 640$  eV from the  $\sim 100$  ppm of Mn is well separated from the dominant O K line at 525 eV, although the resolution is reduced to  $\sim 15$ -20 eV for the larger  $200\ \mu\text{m} \times 200\ \mu\text{m}$  pixels (figure 3, left).

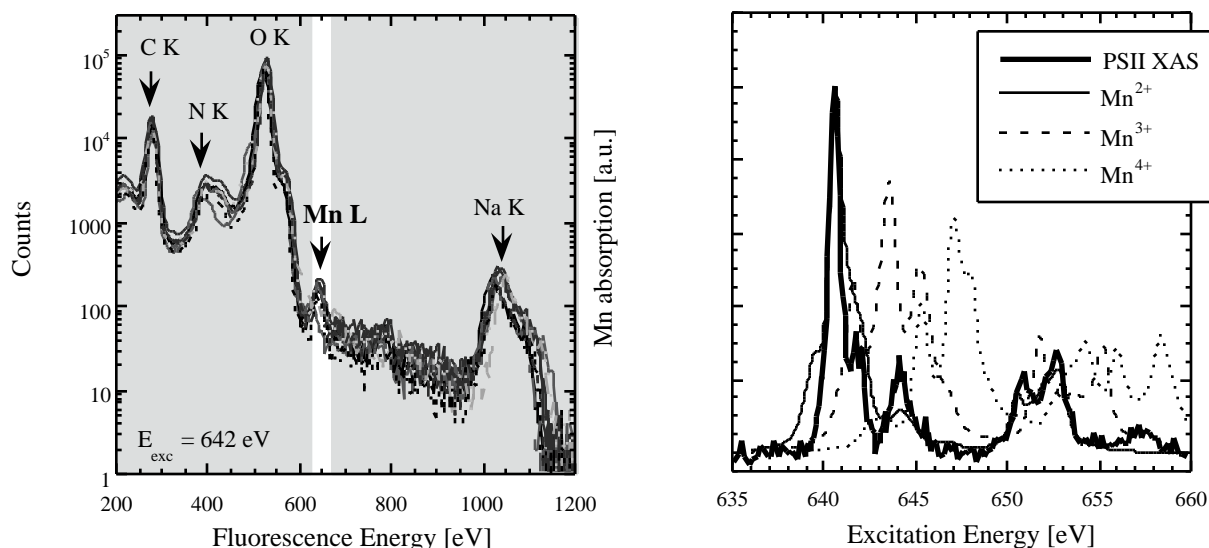


**FIGURE 3.** Left: Fluorescence spectrum from a dried and biologically inactive photosystem II protein showing the response for the nine different pixels in the array. Right: Fluorescence-detected Mn L-edge absorption spectrum of this sample (solid lines), and multiplet calculations of the expected change of the spectrum for Mn in the oxidation state +3 and +4 (dashed lines).

The absorption spectrum is an average of two 50 minutes scans, normalized by the incident beam, with the background subtracted. The spectrum has a  $S_{p-p}/N_{rms}$  ratio of  $\sim 50$ , which is sufficient to determine oxidation states (figure 3, right). The sharp peak at  $\sim 640$  eV is indicative on  $Mn^{2+}$ , not surprising given that the sample is no longer active and  $Mn^{2+}$  is the most stable oxidation state. For comparison, we show the chemical shifts of the absorption spectra expected if all Mn atoms were in the oxidation state +3 or +4. While no biological information should be extracted from these spectra, they illustrate the capabilities of cryogenic STJ detectors for synchrotron-based fluorescence-detected soft X-ray absorption spectroscopy to determine chemical states of dilute samples.

## ACKNOWLEDGMENTS

We gratefully thank J. D. Batteux for his expert technical work, and A. T. Young and E. Arenholz for valuable assistance with the beam line operation. Funding was provided by NIH GM-44380, DOE OBER and NSF DMR 0114216. This work was performed under the auspices of the U.S. Department of Energy by University of California Lawrence Livermore National Laboratory under contract No. W-7405-Eng-48. Disclaimer: This document was prepared as an account of work sponsored by an agency of the United States Government. Neither the United States Government nor the University of California nor any of their employees, makes any warranty, express or implied, or assumes any legal liability or responsibility for the accuracy, completeness, or usefulness of any information, apparatus, product, or process disclosed, or represents that its use would not infringe privately owned rights. Reference herein to any specific commercial product, process, or service by trade name, trademark, manufacturer, or otherwise, does not necessarily constitute or imply its endorsement, recommendation, or favoring by the United States Government or the University of California. The views and opinions of authors expressed herein do not necessarily state or reflect those of the United States Government or the University of California, and shall not be used for advertising or product endorsement purposes.

## REFERENCES

1. For a recent overview of the field, see "Proceedings of the 9<sup>th</sup> International Workshop on Low Temperature Detectors" (LTD-9), AIP Conference Proceedings 605, edited by F. S. Porter, D. McCammon, M. Galeazzi, C. K. Stahle, New York (2002)
2. D. A. Wollman, K. D. Irwin, G. C. Hilton, L. L. Dulcie, D. E. Newbury, J. M. Martinis, J. Microscopy 188, 196-223 (1997)
3. V. Lordi, V. Gambin, S. Friedrich, T. Funk, T. Takizawa, K. Uno, J. S. Harris, Phys. Rev. Lett. 90, 145505-145508 (2003)
4. S. Friedrich et al., J. of Electron Spectroscopy and Rel. Phenomena 101, 891-896 (1999)

5. C. Arnaboldi et al., Physics Lett. B 557, 167-175 (2003)
6. A. Peacock et al., Nature 381, 135-137 (1996)
7. M. Frank et al., Rev. Sci. Inst. 69, 25-31 (1998)
8. S. Friedrich et al., IEEE Trans. Appl. Supercond. 9, 3330-3333 (1999)
9. S. Friedrich, M. F. Cunningham, M. Frank, S. E. Labov, S. P. Cramer, Nucl. Inst. and Meth. A 444, 151-155 (2000)
10. S. Friedrich et al., Nucl. Inst. and Meth. A 467, 1117-1120 (2001)
11. C. Hagmann and P. L. Richards, Cryogenics 34, 221-225 (1994)
12. J. B. LeGrand, et al., Appl. Phys. Lett. 73, 1295-1297 (1998)
13. J. Jaclevic, J. A. Kirby, M. P. Klein, G. S. Brown, and P. Eisenberger, Solid State Comm. 23, 679-682 (1977)
14. A.T. Young, J. Feng, E. Arenholz, H. A. Padmore et al., Nucl. Inst. Meth A 467-468, 549-552 (2001)